Measurements of large-scale circulations in mixed convection in a pressurized model room

M. Herzberg, C. Resagk*, C. Cierpka
Institute of Thermodynamics and Fluid Mechanics, Technische Universität Ilmenau, Germany
* Correspondent author: christian.resagk@tu-ilmenau.de

Keywords: PIV measurements, generic passenger cabin, indoor airflow, large-scale circulations, small-scale model experiment

ABSTRACT

The velocity field of the large-scale circulations (LSC) in turbulent mixed convection is analyzed by means of 2D2C particle image velocimetry (PIV). The experiments are carried out in a small-scale model room resampling a generic passenger cabin. To achieve wide ranges of dimensionless numbers, pressurized dry air is used in the SCALEX (Scaled Convective Airflow Laboratory EXperiment) facility. Three different LSCs have been found, depending on the Archimedes number Ar. The experiments were carried out at air pressures of 1 bar, 5 bar and 9 bar and represent scaling factors of 1, 3 and 4, respectively.

1. Introduction

Large-scale circulations (LSC) in indoor air flows have a major impact on thermal comfort and energy efficiency, as well as for the distribution of pollutants and aerosol particles in passenger cabins, e.g. in airplanes and trains. In order to ensure an ergonomic, safe and energy efficient high-level air quality for every passenger, the formation of this large-scale circulations in thermally and mechanically driven indoor airflows has to be understood. The LSC of airflows in passenger cabins result from mixed convection, i.e. the temporal and spatial superposition of forced and natural convection. Forced convection is mainly characterized by the Reynolds number Re and the natural convection is described by the Rayleigh number Ra. Furthermore, the Prandtl number *Pr*, which describes the ratio between viscosity and thermal diffusivity of the working gas. These dimensionless numbers are defined as:

$$Re = \frac{\rho u_{\mathrm{in}} H}{\eta}$$

$$Ra = \frac{\rho^2 \beta c_p g \Delta T H^3}{\eta \lambda}$$

$$Pr = \frac{\eta c_p}{\lambda}$$

with ρ, β, η, λ, c_p as the working gas density, thermal expansion coefficient, dynamic viscosity, thermal conductivity and thermal capacity, respectively. The inlet velocity is denoted u_{in}, H is the height of the generic passenger cabin, g is the acceleration due to gravity and ΔT denotes the global temperature difference between the aluminum heating blocks and the cooled inlet flow. The ratio of forced convection to natural convection is described by the Archimedes number Ar, which is the ratio of inertial transport of natural and forced convection and reads

$$Ar = \frac{Ra}{PrRe^2} = \frac{\beta g \Delta T H}{u_{\mathrm{in}}}.$$

The evolution of coherent structures (LCS) has been found already in numerical simulations [Bailon-Cuba 2012], but the experimental validation has not been made until now.

2. Experiment

A generic passenger cabin has been used, to investigate the large-scale circulations. The shape of the generic passenger cabin approximates a typical configuration of the cabin of an aircraft or a train. Depending on the working gas and its pressure scaling factors *m (reference length/model length)* of 1, 3, 4 and 8 are achievable (Figure 1). The geometry has a rectangular *xy*-cross-section with length L=0.4 m and height H=0.3 m, as shown in Figure 2. The depth of the model is D=0.5 m. At the top of the generic passenger cabin two opposed gas inlets are arranged. The cooled working gas, which is prepared with an air conditioning system, enters the generic passenger cabin with the inlet velocity u_{in} and the inlet temperature T_{in}. The applied volume flow leaves the cabin through the two opposed outlets that are arranged at the bottom. All side walls are made of Plexiglas in order to achieve optical access to the interior. Furthermore, the generic passenger cabin consists of four aluminum heating blocks that represent the passenger rows and their thermal load.

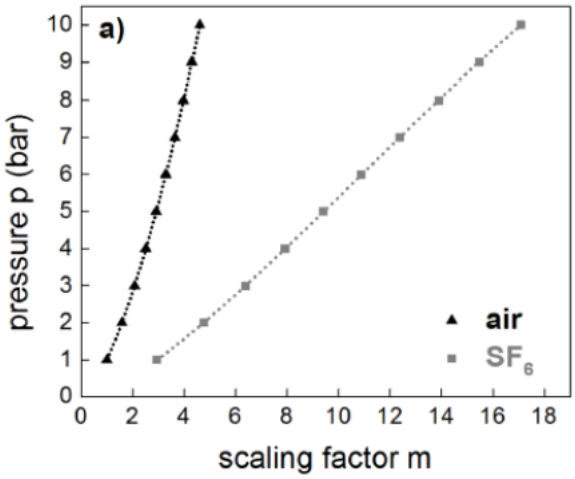

Fig. 1 Scaling factor (based on Ra) depending on working gas and working gas pressure.

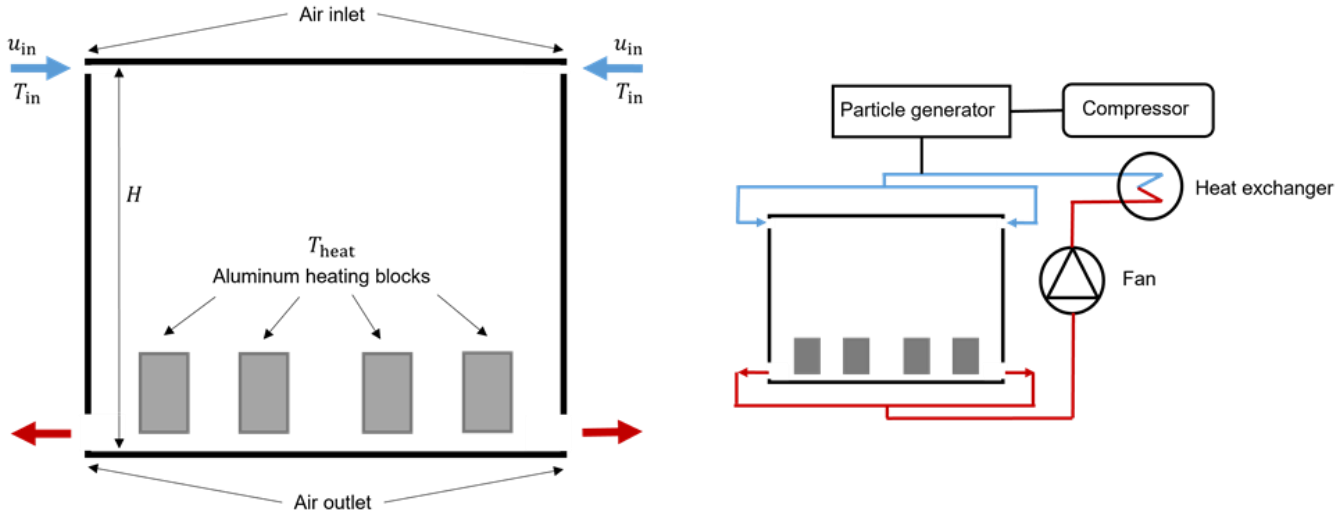

Fig. 2 Schematic of the generic passenger cabin, the arrows mark cold working gas inlet (top, blue) and outlet (bottom, red) (left side) and schematic of the air conditioning system of the generic passenger cabin (right side).

In order to achieve wide ranges of the dimensionless numbers *Re* and *Ra*, the SCALEX facility, shown in Figure 3 is used. This facility consists of a pressure vessel and a working gas supply. The working gases dry air or sulphur hexafluoride (SF_6) isothermally compressed up to p_{max}=10 bar can be used for achieving various ranges of Rayleigh and Reynolds numbers just by modifying the working gas density at room temperature. The Prandtl number remains nearly constant. The implementation of several windows allows the application of optical flow measurement methods like the particle image velocity technique. More detailed information of the generic passenger cabin and the SCALEX facility can be found in [Körner 2013 and 2014].

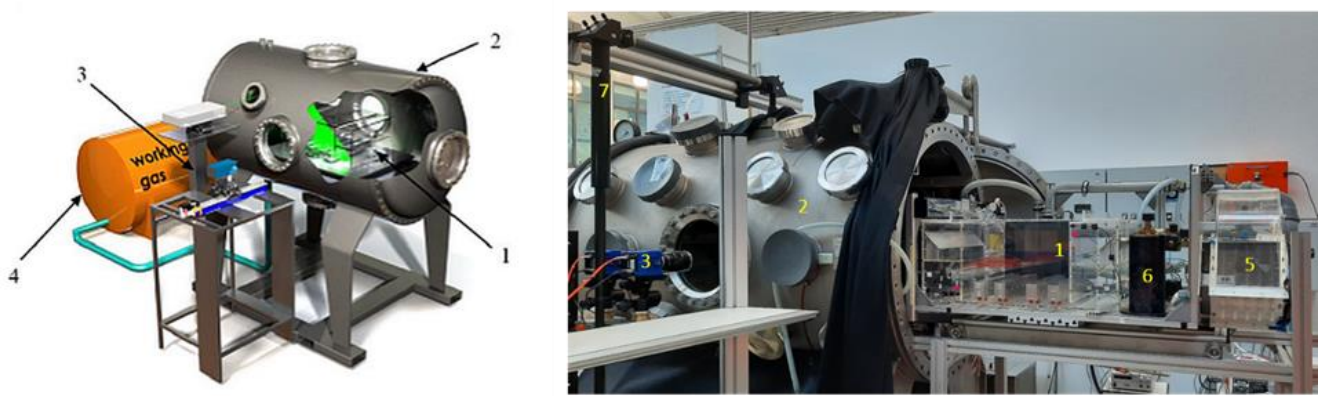

Fig. 3 Schematic of the SCALEX facility (left) and photograph of the experimental setup (right), with: (1) the generic passenger cabin, (2) pressure vessel, (3) sCMOS cameras, (4) working gas supply, (5) heat exchanger, (6) particle generator, (7) laser light sheet optics.

In order to conduct velocity field measurements a 2D2C Particle Image Velocimetry (PIV) system is used. The fluid is seeded with tracer particles which are able to follow the flow. The fluid with tracer particles is illuminated by a laser light sheet and the motion of the seeding particles is used to calculate speed and direction of the velocity field using cross-correlation methods, see [Raffel 2018]. The system consists of a double-pulsed Nd:YAG-laser Q-smart Twins (Quantel), two sCMOS cameras LaVision Imager sCMOS and a programmable timing unit from LaVision GmbH. The laser is equipped with a frequency doubling unit and works at a wavelength of λ=532 nm and a maximum pulse energy E=380 mJ. The camera's resolution is 2560 pixel ×2160 pixel with a pixel size of 6.5 µm ×6.5 µm. They are located next to each other to extend the field of view (FOV) to the whole generic passenger cabin, shown on the right side of Figure 3. The magnification is 0,12 mm/pixel. The tracer particle generator (PIVpart12 from Pivtec GmbH) is implemented in the air conditioning system inside the SCALEX and provides Di-ethyl-hexyl-sebacat (DEHS) particles atomized to an average particle size of d_p≈1 µm. The laser and the cameras are located outside of the pressure vessel, depicted on the left side of Figure 4. The raw data from the PIV system is evaluated using advanced double-frame based PIV-algorithms implemented in the software Davis 10 from LaVision GmbH. The final interrogation window size has been chosen to be 48 pixels × 48 pixels with an overlap of 50 %. The vector field resolution is 2.95 mm × 2.95 mm in the laboratory scale. This corresponds to a resolution of 29.5 mm × 29.5 mm for a room in the original scale with Dimension of height H=3 m.

3. Results and discussions

Three different structures of the LSC within the generic passenger cabin can be reported and are depicted in Figure 5. The figures show the measured instantaneous velocity fields, the time averaged vector plots, the time averaged vorticity and the root mean square (rms) value of the velocity field in the xy-plane in the middle of the generic passenger cabin.

At a low Ar number the flow is dominated by forced convection. The velocity distribution in this case is characterized by two counter-rotating large vortices left and right of the middle of the generic passenger cabin. This LSC is depicted in the first column of Figure 4. The related measurement is performed at an Archimedes number of Ar = 0.18, a Rayleigh number of Ra = 2.36 $\cdot 10^7$ and a Reynolds number of Re = 1.39 $\cdot 10^4$. Based on the fact, that the temperature of the inflow air is lower than the mean temperature within the generic passenger cabin, the flow is strongly directed downwards against the buoyancy flow from the aluminum heating blocks. This LSC is

highly turbulent as indicated in the instantaneous velocity field in the first row of Figure 5. In the rms plot the highest fluctuation occurs at the position, where the two wall jets meet each other.

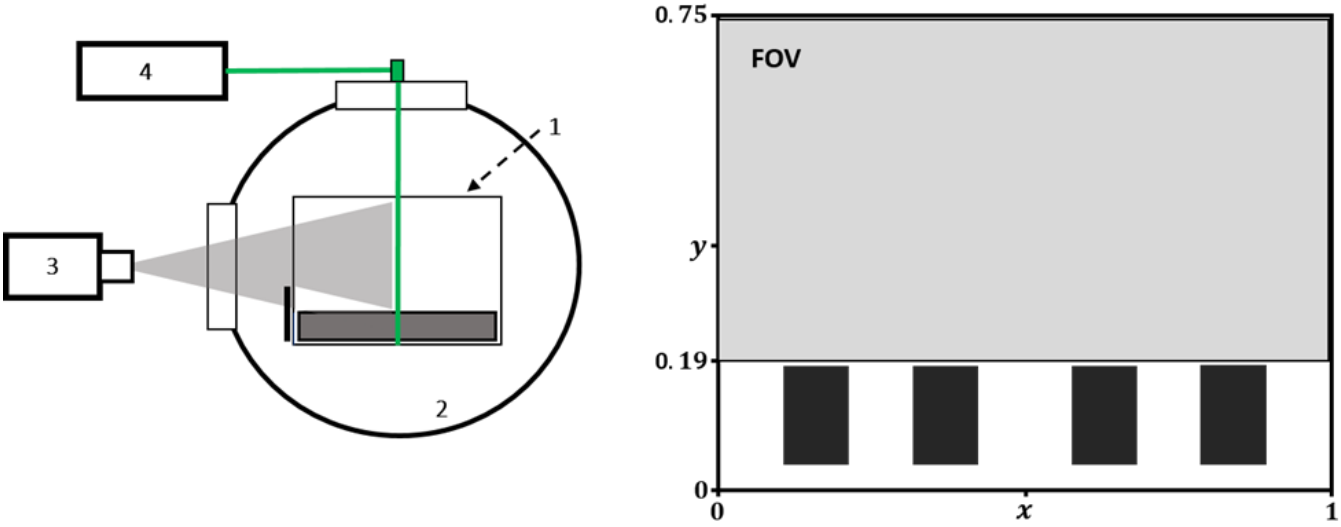

Fig. 4 Principle of the PIV setup (left) with: (1) generic passenger cabin, (2) SCALEX pressure vessel, (3) sCMOS cameras, (4) laser with laser light sheet (green) and the field of view (right) inside the generic passenger cabin.

The Archimedes number increases with decreasing inlet velocity u_{in} at a constant temperature difference ΔT. At an Archimedes number of Ar=0.5, with the corresponding Rayleigh and Reynolds numbers of $2.64 \cdot 10^7$ and $8.55 \cdot 10^3$, respectively, the flow is near the equilibrium of forced and natural convection. In this case, one of the vortices become dominant and a one-roll-system with the main rotation axis in z-direction is formed. A smaller secondary vortex with higher vorticity can be found on the opposite inlet.

At high Archimedes numbers the flow is dominated by natural convection. The behavior of the flow shows a strong influence of buoyancy over the whole cabin cross-section. The related measurement is performed at an Archimedes number Ar=3.4 with a Rayleigh and Reynolds number of $2.54 \cdot 10^7$ and $3.48 \cdot 10^3$, respectively. At the side walls of the generic passenger cabin a wall-bounded flow downwards to the outlet can be found. In the vorticity plot, a change in the sign of the vorticity can be seen on both sides. From the velocity distribution it is clear, that in the considered cross-section more air is flowing upwards, than downwards. With respect to the mass conservation law, this is a hint for a more three-dimensional character of the flow field with a pronounced z-component.

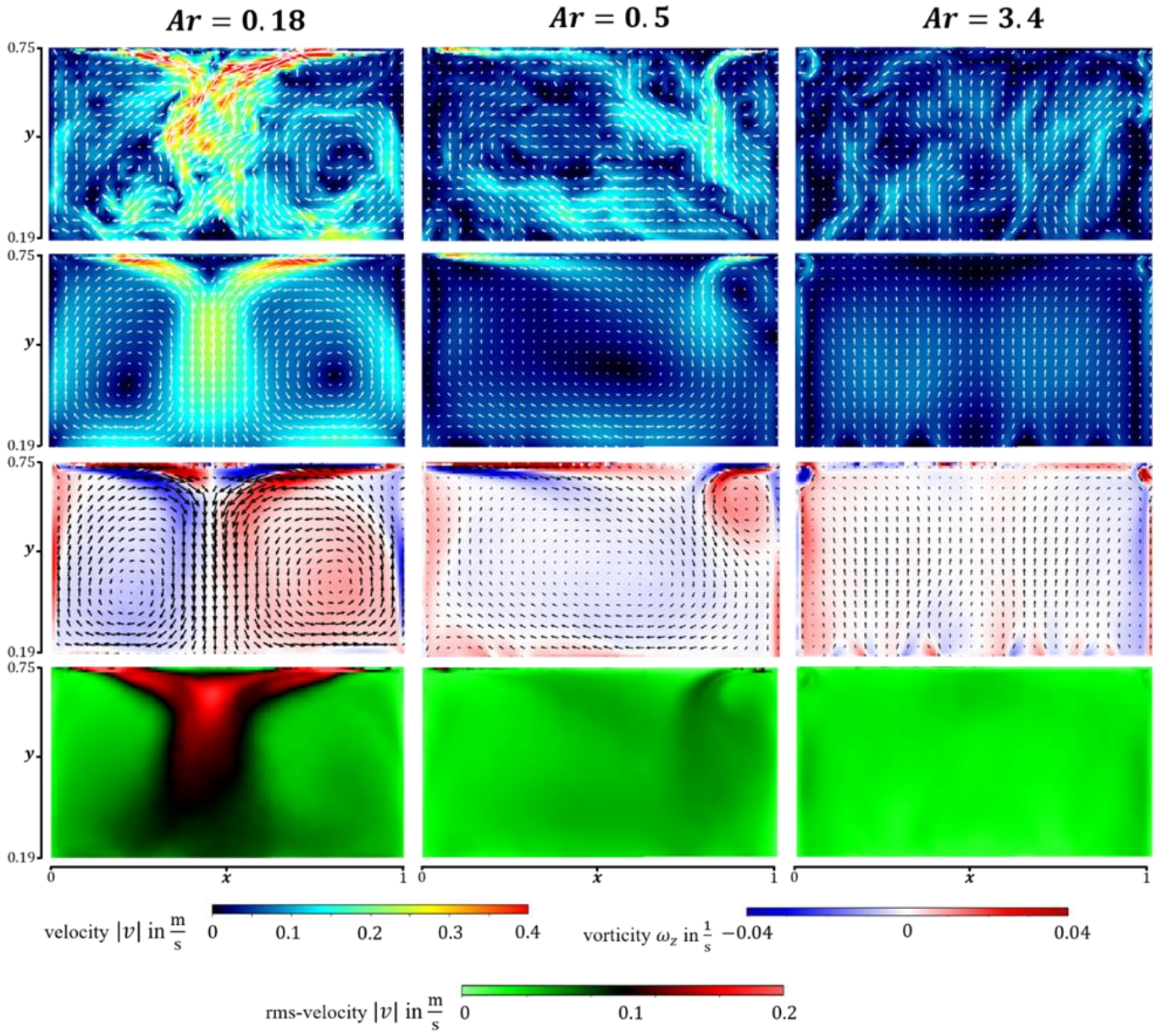

Fig. 5 Instantaneous (first line), time averaged (second row) and root mean square (third row) velocity vector field and vorticity plot (fourth row) for three different Archimedes numbers Ar=0.18, Ar=0.5 and Ar=3.4 at Ra=2.5·10^7 (only every fourth vector shown). This investigation was carried out with air at 1 bar.

By increasing the pressure inside the SCALEX facility up to 5 bar, it is possible to increase the Rayleigh number as an important milestone in direction of high-pressure SF6 measurements. In Figure 6 first preliminary measurement results at a Rayleigh number of Ra=7.8·10^8 and Re=6.86 ·10^4 are depicted. The measurements were carried out at an Archimedes number of Ar=0.23. The structure reminds on the LSC in the first row of Figure 5. But it seems that the right side of the inlet flow becomes more dominant. The two inlet wall jets meet each other in the middle of the generic passenger cabin and form a diagonal jet in direction of the left air outlet. On the left side

of the cabin, the rms-value is higher. That's indicates a higher turbulence on this side and a transition to a different LSC.

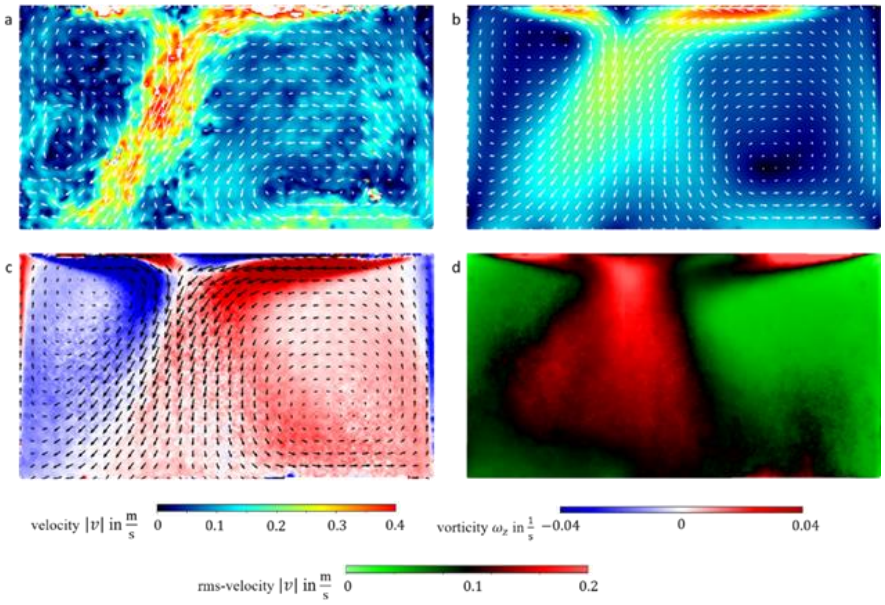

Fig. 6 Instantaneous (a), time averaged (b) and root mean square (d) velocity vector field and vorticity plot (c) for Archimedes number Ar=0.23 at Rayleigh number Ra=7.8·10^8 and Re=6.86 ·10^4 (only every fourth vector shown), carried out with pressurized air at 5 bar.

Fig. 7 shows the preliminary measurement results for a Rayleigh number of Ra=2.5·10^9. The measurements were carried out at Archimedes numbers of Ar=0.18, Ar=0.5 and Ar=3.4. The basic structures reminds on the LSCs shown in Fig. 5. At the lower Archimedes number of Ar=0.18 it seems that the turbulence on the right upper side of the chamber becomes even higher.

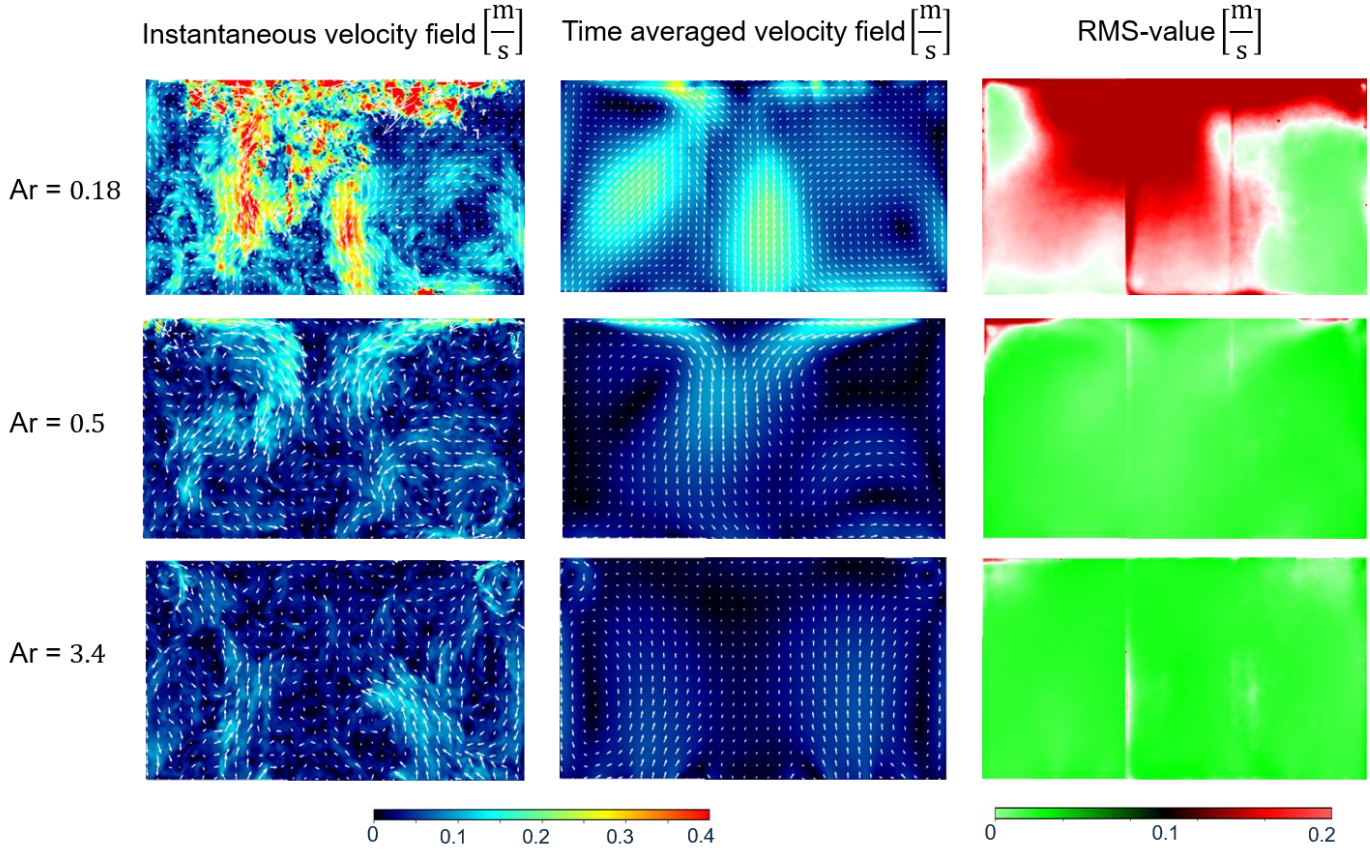

Fig. 7 Instantaneous (a), time averaged (b) and root mean square (d) velocity vector field and vorticity plot (c) for Archimedes numbers Ar=0.18, Ar=0.5 and Ar=3.4 at Rayleigh number Ra=2.5·10^9 (only every fourth vector shown), carried out with pressurized air at 9 bar.

4. Conclusions

In this proceeding a model experiment has been shown, that allows the investigation of LSC within a generic passenger cabin. This setup consists of a small-scaled model room, the SCALEX facility and a high-resolution particle image velocimetry system.

It has been shown that in generic passenger cabins different LSCs occur in the mean flow, depending the Archimedes number Ar. For more detailed investigations, a stereoscopic particle image velocimetry technique in different cross-sections over the depth of the cabin are planned that come with their own challenges [Cierpka 2019]. Furthermore, for a similarity with cabins in full scale, measurements using SF6 are needed. The results of measurements at higher Archimedes numbers in Figure 5 represent a first intermediate step to achieve full similarity. More detailed results will be presented in the talk.

A better knowledge of the different LSCs, will help to optimize the thermal behavior and the air quality in passenger cabins. Furthermore, it can contribute to reducing the spread of aerosols and leads to a better understanding of infection events of COVID-19.

Acknowledgement

Financial support from Deutsche Forschungsgemeinschaft (DFG) for the framework of the research projects RE 1066/20-1 and CI 185/10-1 is gratefully acknowledged. The authors would also like to thank Alexander Thieme for technical support.

References

Bailon-Cuba, J., Shiskina, O., Wagner, C., Schumacher, J. (2012). Low-dimensional model of turbulent mixed convection in a complex domain. *Physics of Fluids,* 24, 107101

Körner, M., Shishkina, O., Wagner, C., Thess, A. (2013). Properties of large-scale structure in an isothermal ventilated room. *Building and Environment*, 59, 563-574

Körner, M. (2014). Experimental method for the investigation of indoor airflows in a reduced scale model room: development and application. *PhD Thesis*, *Technische Universität Ilmenau*

Raffel, M., Willert, C. E., Scarano, F. (2018). *Particle Image Velocimetry - A Practical Guide*, Third edition. Springer International Publishing

Cierpka, C., Kästner, C., Resagk, C., Schumacher, J. (2019). On the difficulties for reliable measurements of convection in large aspect ratio Rayleigh-Bénard cells, *Experimental Thermal and Fluid Science*, 109, 109841, DOI: 10.1016/j.expthermflusci.2019.109841